Sofia University "St. Kliment Ohridski"

Physics Faculty

Luminosity measurements at CMS

A thesis submitted for the degree of Bachelor of Physics

by Peter Tsrunchev

Thesis advisor:
Dr. Anne Dabrowski

Thesis Consultant:
Prof. Dr. Leandar Litov

November 5, 2018

Acknowledgements

First and foremost I want to express my deepest gratitude to my supervisors Dr. Anne Dabrowski, Dr. David Stickland and Dr. Olena Karacheban who all guided me throughout my time at CERN for all the patience, support and advice they have given me over the past year and a half.

I also want to thank Dr. Moritz Guthoff who first brought me into the BRIL project, Dr. Nicolò Tosi who was a great office mate and all-round walking encyclopedia, and everybody else at BRIL and building 598 for being awesome and making working there so wonderful.

Thanks also to Prof. Dr. Leandar Litov for consulting on this thesis.

Lastly, I'd like to thank my parents Delyana Tsruncheva and Tsvetelin Tsrunchev for always being there and pushing me to be better. I especially want to thank my father for all the long late night discussions while I was writing this thesis.

Abstract

The topic of this thesis are the methods used for luminosity measurements at the CMS experiment, focusing on calibration of luminometers using Simon van der Meer's method and using so-called "emittance scans" in various studies.

The thesis starts with a brief introduction to the Large Hadron Collider (LHC), the Compact Muon Solenoid (CMS) experiment and their purpose. The concept of luminosity fixed target and colliding beams experiments is discussed. The different luminosity detectors at CMS are described. The Van der Meer (VdM) scan method is described accompanied by a modern theoretical derivation assuming Gaussian beams and a brief outline of the various corrections and systematic uncertainties applied post-calibration. An extensive report on the software framework used in VdM analysis at CMS is done - for both the previously used (although optimized) core version and its automated wrapper.

The final chapter discusses the use of "emittance scans" - short VdM-like scans at the beginning and end of every fill - for luminosity calibration. A novel, self-contained (non-reliant on comparison to other detectors) method for non-linearity estimation using those scans is discussed, as well as their further use for long term stability monitoring.

Contents

Chapter 1

Introduction

1.1 The Large Hadron Collider

The Large Hadron Collider (LHC)[1] is the largest particle accelerator collider in the world. Its circumference spans 27 km in the French and Swiss countryside near Geneva, between 45 m and 170 m underground. The tunnel was constructed for the Large Electron Positron (LEP)[3] collider in 1984-1989. The beams rotate in opposite directions along two parallel beam pipe rings and gets accelerated by radio frequency (RF) cavities in which the electromagnetic field oscillates at 400 MHz.

The LHC machine is designed to accelerate two proton beams moving in opposite directions from 450 GeV to 7 TeV and then collide them at four interaction points (IPs), around which the four big experiments on the LHC are built - ATLAS, ALICE, CMS and LHCb. At these energies the protons in the beam complete 11245 orbits around the LHC. This and the RF cavities frequency determine the harmonic number of the LHC to be 35640[4]. This is the number of virtual positions (buckets) in the LHC circumference that could be filled with particles to be accelerated. The beams are separated into 25 ns-spaced bunches, making for a total 3564 bunch slots. Some of these are reserved for the abort gap - the time needed for the beam dumping magnets to kick in. The LHC gets filled with 12 "supercycles" of the 234 bunches in the Super Proton Synchrotron (SPS) [5]. The maximum number of occupied buckets or bunches in the LHC is 2808. Each bunch contains around 1.15×10^{11} protons at the start of a nominal fill.

The initial proton beams are prepared by a series of accelerator facilities on the CERN site (Figure 1.1). First the linear accelerator LINAC 2 accelerates protons up to 50 MeV, then the Proton Synchrotron Booster accelerates them to 1.4 GeV and

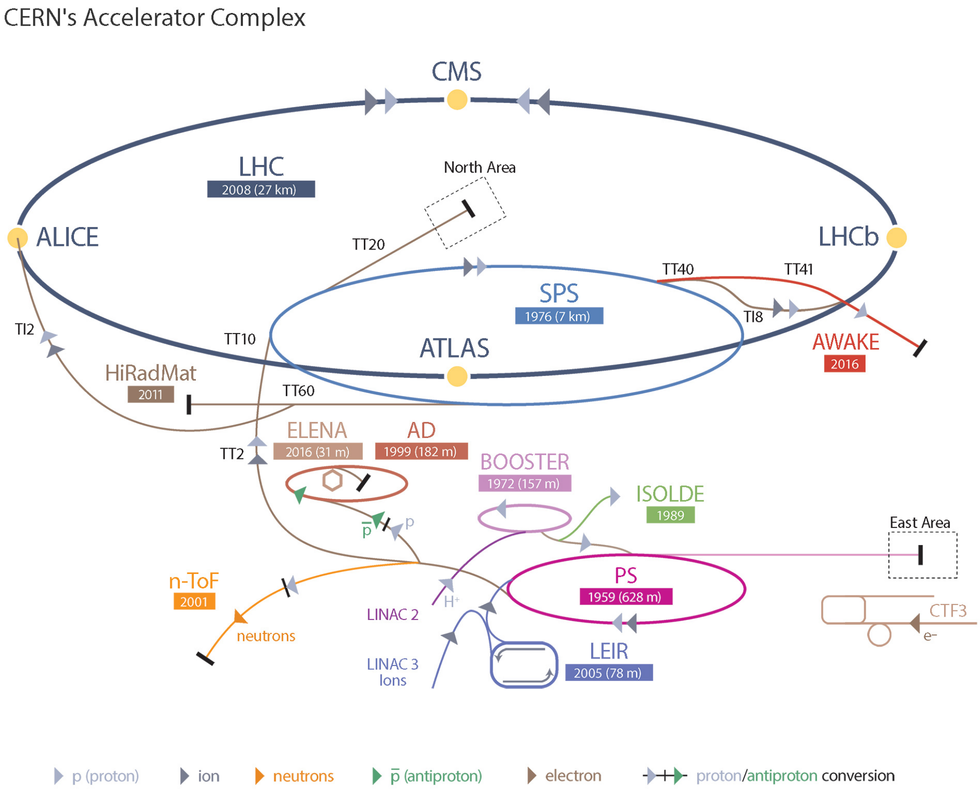

Figure 1.1: CERN Accelerator complex schematic

injects them into the Proton Synchrotron (PS), where they are further accelerated to 26 GeV before finally reaching the Super Proton Synchrotron (SPS), which accelerates them to 450 GeV. For about a month each year the LHC also accelerates and collides heavy ions - lead-lead, proton-lead, or most recently - xenon-xenon. The maximum center-of-mass energy achieved is 5.02 TeV per colliding nuclear pair for lead[6] and 5.44 TeV per colliding nuclear pair for xenon[7].

The main goal of the LHC project was to test various predictions and theories of particle physics, mainly deciding between the Standard Model and some other Higgsless model to explain the electroweak symmetry breaking giving mass to the W and Z bosons. On July 4th 2012 in a joint announcement the ATLAS and CMS experiments confirmed they had both observed a particle with a mass around 126 GeV that was consistent with the Higgs boson predicted by the Standard model at 5σ significance [8, 9]. Studies in the next years have further shown evidence that this is in fact a Higgs boson. It is not yet certain if this is the Standard Model Higgs boson or one of multiple Higgs bosons from other theories beyond the SM.

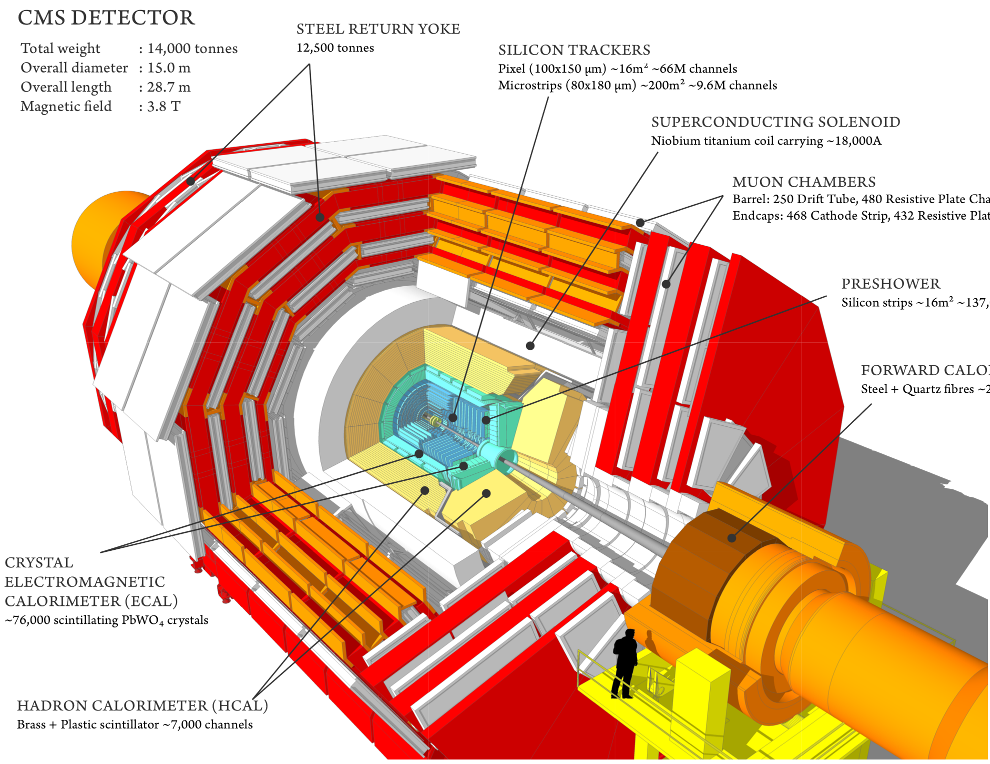

Figure 1.2: CMS Schematic

1.2 The CMS Experiment

The Compact Muon Solenoid[10] (shown in Figure 1.2) is one of the two general purpose experiments at the LHC (along with ATLAS). It is 21 m long and 14.6 m wide and weighs 12500 ton. The detector was designed with requirements for good performance in:

- Muon identification and momentum resolution and unambiguous charge determination when p <1 TeV;
- 1% dimuon, diphoton and dielectron mass resolution at 100 GeV;
- Charged-particle momentum resolution and reconstruction efficiency;
- Electromagnetic energy resolution, geometric coverage, π^0 rejection, and photon and lepton isolation at high luminosities;
- Missing-transverse-energy and dijet-mass resolution.

The coordinate system (Figure 1.3) used in CMS has its x-axis pointing towards the center of the LHC, y-axis pointing vertically upward and z-axis pointing along the beamline. The azimuthal angle ϕ is measured in the x-y plane while the polar angle θ

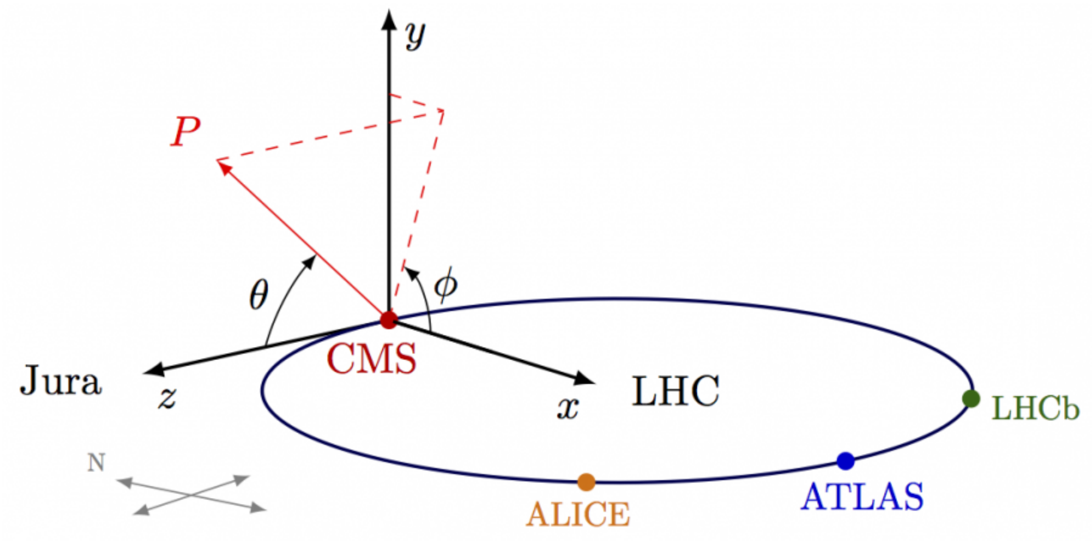

Figure 1.3: CMS coordinate system

is measured from the z-axis. Often in particle physics the parameter pseudorapidity $\eta = \ln(\tan\theta/2)$ is used instead of the latter as it is Lorenz invariant.

Magnet

The namesake of the CMS experiment is the solenoid - a superconducting niobium titanium coil measuring 13 m long and 7 m wide, creating a 3.8 T magnetic field. This is needed to curve the trajectory of high energy particles, allowing the measurement of their momentum.

Tracker

The innermost part of the CMS is the tracking system comprised of multiple layers of silicon pixel (100 µm × 150 µm) and silicon strips (80 µm × 180 µm) modules. They measure the positions of passing charged particles, which are used to reconstruct the particle trajectories, giving their momenta.

Calorimeters

The calorimeters are designed to absorb and measure the energy of as many particles as possible. There are two calorimeters - the Electromagnetic Calorimeter (ECAL) and the Hadronic Calorimeter (HCAL).

ECAL Next come the calorimeters which measure the energies of most particles and them. The Electromagnetic Calorimeter (ECAL) deals with electrons and photons. It is made from $PbWO_4$ scintllating crystals which are read out with Avalanche Photo

Detectors and covers pseudorapidity up to $|\eta| < 3.0$. In the endcaps there is also a preshower system of smaller (2 mm compared to 3 cm wide) Si-Pb sensors for π^0 diphoton decay rejection.

HCAL The Hadronic Calorimeter (HCAL) is built from alternating layers of brass (absorber) and plastic scintillators. Hadrons may interact with the absorber producing multiple secondary particles which then also interact, resulting in a "shower" of particles. These then pass through the alternating layers causing scintillation which is then transferred to strategically placed readout boxes through tiny optical "wavelength-shifting fibres" and clear optic tables. Multiple layers that are chosen so they receive roughly the same number of particles get optically added to form "towers". This allows for energy measurements. The HCAL can also be used to deduce production of otherwise undetectable particles (e.g. neutrinos) from imbalance in the momentum and energy measured along the transverse direction.
HCAL is the outermost part of the detectors that is still inside the solenoid, but it also has several additional layers just outside the magnet (HO, outer barrel). The rest of it is organised into the barrel (HB), endcap (HE) and forward (HF) sections, each covering a different range of pseudorapidities, the latter going as high as $|\eta| = 5.0$. The HF is also used for luminosity measurements as described in subsection 2.3.4.

Muon chambers

An iron yoke outside the magnet is employed to guide and contain the magnetic field. It is interleaved with the muon detectors in three layers spanning out 14 m in diameter. Only muons and weakly interacting particles pass through the calorimeters and the "return yoke".
The outermost part of the CMS detector is the muon chambers designed to identify muons and measure their momentum. It is crucial to the search for the Higgs boson as the ZZ and ZZ* decay channels can further decays into four muons which allow for the best mass resolution as they are less susceptible to radiation losses.

The Drift Tube (DT) system is deployed in the barrel, where background levels are low, covering $|\eta| < 1.2$. Each tube is 4 cm wide and contains a stretched wire in a gas volume. When a charged particle passes it ionizes the gas and the resulting electrons get pulled by the field to the positive wire. The time it takes for the electron to reach the wire combined with the position along the wire where it hits gives two coordinates of the particle's position.

The Cathode Strip Chambers (CSCs) are employed in the endcaps, where there are high muon and background rates, $0.9 < |\eta| < 2.4$. They are arrays of positively charged wires crossed with negatively charged ones within a gas volume. Charged particles again knock electrons towards the anodes and ions toward the cathodes, giving two coordinates per detection.

The Resistive Plate Chambers (RPCs) provide a fast, robust and independent trigger system parallel to those of the other two muon systems ($|\eta| < 1.6$), but with worse position resolution. They consist of two parallel oppositely charged high-resistance plates separated by gas. Muons cause electron avalanches in the gas which after a precise time delay get picked up by external metallic strips.

Chapter 2

Luminosity measurements at CMS

2.1 Definition of luminosity

Cross section for beam-target interaction

When a particle beam of density n_1 and velocity $\vec{v}_1$ hits a target with particle density n_2, the density of the interaction rate can be expressed as

$$\frac{\partial^2 N}{\partial V \partial t} = \sigma_{int} |\vec{v}_1| n_1 n_2. \tag{2.1}$$

The parameter σ_{int} is called the interaction cross section. It carries the probability for that interaction and has the units of area - either cm^2 or $\mathrm{b} = 10^{-28}\,\mathrm{cm}^2$. The total collision cross section (for all possible events) corresponds to the probability of collision. The term cross section was first coined in times when particles were thought of as solid spheres, making the probability of their collision dependent on their actual physical cross sections.

Luminosity of a stationary target collider

Equation 2.1 can be expressed as

$$\frac{\mathrm{d}N}{\mathrm{d}t} = \iiint_V \sigma_{int} |\vec{v}_1| n_1 n_2 \,\mathrm{d}x\,\mathrm{d}y\,\mathrm{d}z = \mathcal{L}\sigma_{int}, \tag{2.2}$$

where $\mathcal{L}$ is the instantaneous luminosity - a global measure of the event rate. It is measured in $\mathrm{cm}^{-2}\,\mathrm{s}^{-1}$ or $\mathrm{b}^{-1}\,\mathrm{s}^{-1}$. Knowing one interaction cross section and measuring its event rate, the luminosity can be obtained. Cross sections for other interactions can then be determined from their event rates. Measuring luminosity only requires an apparatus that counts a quantity linear to the number of interactions (and therefore to luminosity), in other words can measure a rate

$$R = \mathcal{L}\sigma_{vis}, \tag{2.3}$$

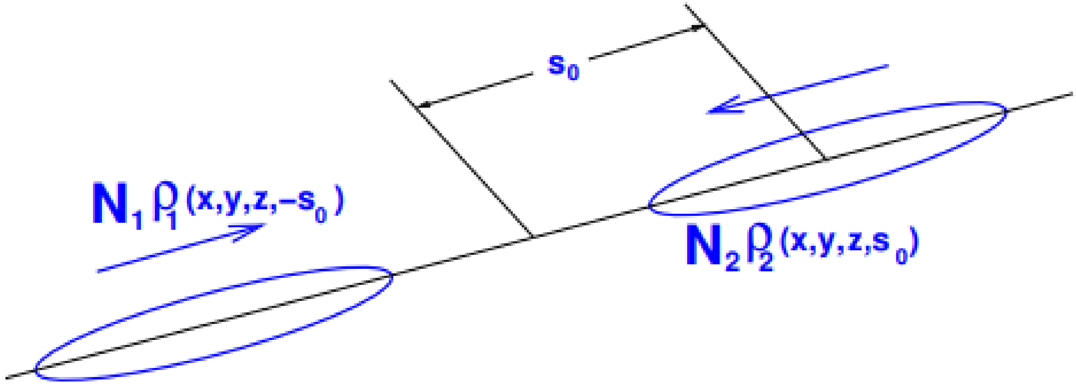

Figure 2.1: Colliding bunches time parametrization

where the linear coefficient σ_{vis} is called the visible cross section of the detector and is dependent on the size, position relative to the interaction point, and active material of the device. The calibration of an instrument for luminosity measurements (luminometer) consists of the estimation of this constant.

2.2 Luminosity of colliding beams

Head-on collisions of non-bunched beams

The density of the interaction rate of two colliding bunches with particle densities n_1 and n_2 and velocities $\vec{v}_1$ and $\vec{v}_2$ was derived by W.C. Middelkoop and A. Schoch[11] using both a coordinate transformation and a more elegant Lorentz invariant formulation first described by Møller[12]. The total cross section σ is assumed to be Lorentz invariant:

$$\frac{\partial^2 N}{\partial V \partial t} = \sigma n_1 n_2 \left[(\vec{v}_1 - \vec{v}_2)^2 - \frac{(\vec{v}_1 \times \vec{v}_2)^2}{c^2} \right]^{1/2} . \tag{2.4}$$

This means the luminosity, assuming non-bunched beams, is

$$\mathcal{L} = \iiint_V n_1 n_2 \left[(\vec{v}_1 - \vec{v}_2)^2 - \frac{(\vec{v}_1 \times \vec{v})^2}{c^2} \right]^{1/2} \mathrm{d}x \, \mathrm{d}y \, \mathrm{d}z \, , \tag{2.5}$$

and in the case of head-on collisions ($\vec{v}_1 = -\vec{v}_2$) becomes

$$\mathcal{L} = 2 \iiint_V n_1 n_2 \, \mathrm{d}x \, \mathrm{d}y \, \mathrm{d}z \, . \tag{2.6}$$

Bunched beams

The case of bunched beams warrants the introduction of the accelerator orbit frequency f and the number of bunches per beam N_b, as well as the number of particles

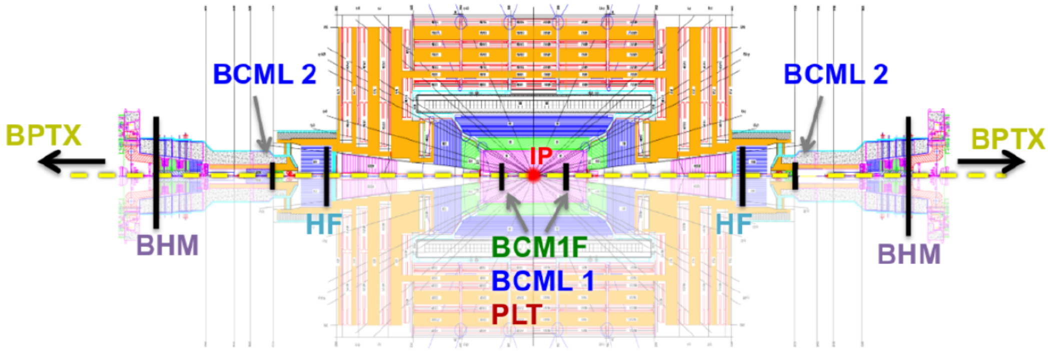

Figure 2.2: BRIL detector positions in CMS

in the colliding bunches N_1 and N_2. The bunched pattern also requires a time dependence. Such can be introduced along the z axis (see Figure 1.3) with the parameter $s_0 = ct$, illustrated in Figure 2.1 Now the expression for luminosity becomes

$$\mathcal{L} = 2N_1 N_2 f N_b \iiiint \rho_1(x_1, y_1, z_1, -s_0)\rho_2(x_2, y_2, z_2, s_0)\, \mathrm{d}x\, \mathrm{d}y\, \mathrm{d}z\, \mathrm{d}s_0\,, \tag{2.7}$$

where $\rho_{1,2}$ are the time dependent beam density distributions.

2.3 Luminometers at CMS

The Beam Radiation Instrumentation and Luminosity (BRIL) [14] project is responsible for luminosity, beam timing and machine induced background (MIB) measurements at CMS. The positions of all the BRIL-operated detectors in the CMS can be seen in Figure 2.2. This thesis is focused on the luminosity measurement aspects of the project's activities.

2.3.1 Offline and Online luminosity

Luminosity measurements are separated by the way they are obtained and analysed. Online luminosity is an initial estimate of instantaneous (or integrated over a short period, e.g. an LHC orbit) luminosity. Detectors providing this measurement need to have fast readout systems allowing for momentary analysis.

Online luminosity provided to CMS and the LHC is used for monitoring purposes and needs to have a reliable and stable system providing it. An independent data acquisition system based on the CMS XDAQ[15] software framework has been developed to allow luminosity measurements even when the central CMS data acquisition system is offline or has problems. Due to their fast readout systems, online luminometers can also separate measurements per bunch crossing (BX), allowing for fine grained monitoring of the beam and bunch train structure studies.

Offline luminosity is usually calculated at the end of the year when all the data is available, including general purpose detectors with more complicated readout systems not optimized for luminosity. This is the most precise measurement, it is corrected for all known effects and used in all physics analyses done by the collaboration. Its precision therefore directly affects the precision of all those results and is of crucial importance.

2.3.2 Zero-counting algorithm

Generally, a luminometer counts or measures a quantity that is linear to luminosity and therefore to the number of primary interactions. However, luminometers often cannot distinguish between a single hit and multiple hits in the same sensor, prompting the use of the so-called "zero counting" method. Since the number of hits should follow a Poisson distribution, the probability of having n hits is

$$p(n) = \frac{\mu^n e^{-\mu}}{n!} \tag{2.8}$$

and so the mean value μ is

$$\mu = -\ln\left(p(0)\right) = -\ln\left(1 - p(\neq 0)\right) \tag{2.9}$$

The probability of having no hits can therefore be used to calculate luminosity, given that the occupancy is low enough.

2.3.3 PLT

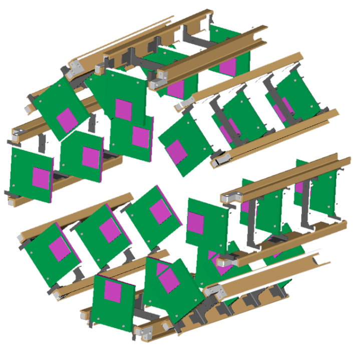

Figure 2.3: Pixel Luminosity Telescope sensor arrangement

The Pixel Luminosity Telescope [16] is a dedicated luminometer using phase-0 CMS pixel sensor detector modules and readout chips. Each module has an active area of 8×8 mm in the x-y plane and 80×52 discrete pixel sensors. The modules are arranged in columns of three along the z axis called telescopes (Figure 2.3) at a total distance of about 7.5 cm, so that a track coming from the interaction point (IP) passes through all three modules. Eight telescopes are installed around the beampipe at a radius of 5 cm just outside each CMS pixel detector endcap (1.75 m from the IP on each side of the CMS) for a total of 16 telescopes (48 sensors). This corresponds to a pseudorapidity of about $|\eta| = 4.2$. A special "fast-or" mode of the readout chip is used, allowing for 40MHz readout (per bunch crossing measurements) by only showing whether any pixels in a sensor were hit. A particle crossing through all three sensors in a telescope indicates a track from the IP and is called a "triple coincidence". The rate of triple coincidences should be proportional to luminosity. The zero-counting method is used here to measure luminosity.

2.3.4 HF

The Hadronic Forward calorimeter (HF) is also used for both offline and online luminosity measurements. It is part of the HCAL (see section 1.2). It is positioned 11.2 m away from the IP on each end of CMS and covers a pseudorapidity range of $3 < |\eta| < 5$, but only the four azimuthal rings with $3.5 < |\eta| < 4.2$ are used for luminosity measurement to minimize non-linear contribution, amounting to 864 towers. Two separate algorithms have been used for HF luminosity measurements:

- **HFOC** - This is the algorithm used in Run 1 and ever since. It uses the zero-counting method on the number of occupied towers in the HF.
- **HFET** - This algorithm was first used in 2017 and was expected to smaller nonlinearity. The main observable here is the sum of all the transverse energy deposited into the HF. It was considered the most reliable and stable throughout the year and so was the offline luminometer of choice for the year.

Lookup tables are used to calibrate ADCs to energy. In the central HF DAQ system these tables are regularly updated, but for luminosity they have been kept constant for each year and corrected by a degradation model provided by HF detector experts.

2.3.5 BCM1F

The Fast Beam Condition Monitor[18] (BCM1F) was first commissioned in 2008 as a machine induced background (MIB) monitor. It is installed in a strategic location at 1.8 m from the IP (right next to the PLT, Figure 2.4) at a radius of 6.94 cm in order to separate incoming MIB and outgoing collision background by 12.5 ns. This, combined with excellent time resolution (6.25 ns) allows the detector to also be used for luminosity measurements, which can be corrected by the background measurement. The detector has been upgraded multiple times since its initial installation and in the 2016-17 Extended Year-End Technical stop it was installed with 10 poly-crystalline chemical vapour deposition (pCVD) diamond sensors, 10 silicon sensors and 4 single crystalline CVD (sCVD) diamond sensors. CVD crystals use two-pad metallization,

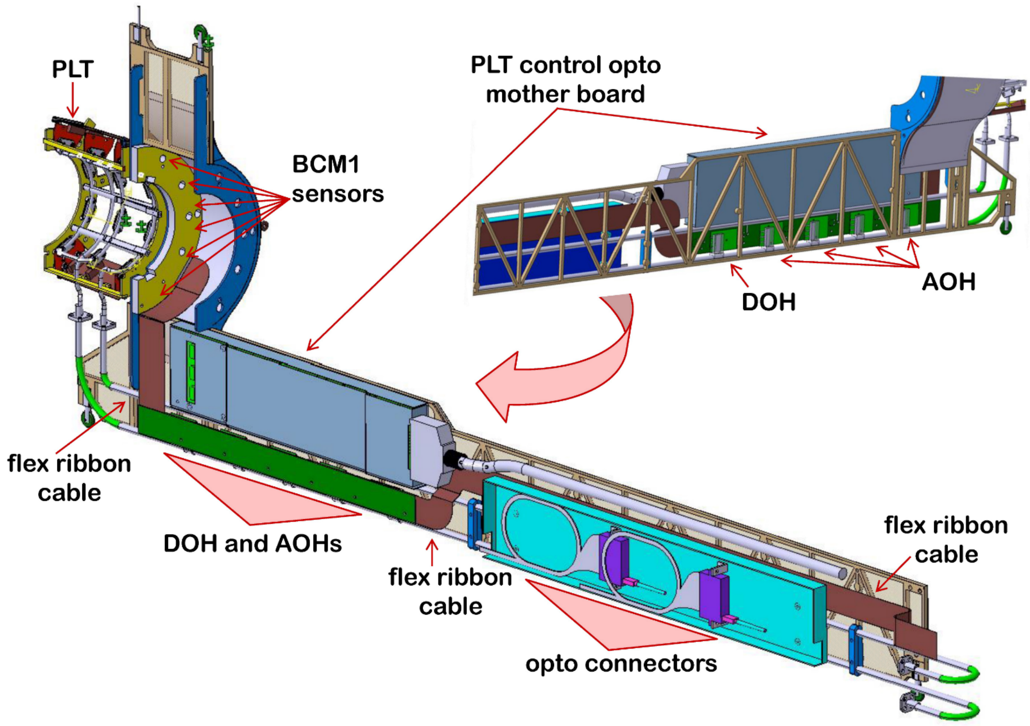

Figure 2.4: BCM1F and PLT carriage

while silicon ones use single pads, making a total of 38 readout channels. Each channel is treated as a separate luminometer using the zero-counting algorithm on the number of hits per bunch crossing.

2.3.6 CMS Tracker

The innermost part of the CMS Tracker is comprised of a total of 66 million separate pixel detectors of size 100 µm × 150 µm. The detector is not suitable for online luminosity monitoring since it is only on when "Stable Beams" have been declared and is reliant on the CMS data acquisition system[19]. The readout system is not designed for online luminosity measurements, but the detector can measure luminosity high precision. For calibration purposes, in order to reach the required statistical precision, only 5 bunches are selected to be read out.

The Pixel Cluster Counting (PCC) [19, 20] method is used for luminosity measurements using the CMS Tracker. It provides a stable and reliable measurement due to the amount of data it provides and was the primary offline luminosity measurement source for 2015 and 2016, but problems in the power supply chain in the last part of the 2017 run significantly reduced the number of used modules. The method is based on the assumption that, since the occupancy in the detector is at the per-mil level, the mean pixel clusters per bunch crossing is proportional to the number of interactions μ which is given by the proton-proton minimum bias cross-section and instantaneous luminosity as

$$\mu = \frac{\sigma_{interaction}}{f}\mathcal{L} \tag{2.10}$$

and, taking the linearity to the average number of clusters $\langle N_{clusters} \rangle$,

$$\mathcal{L} = \frac{\langle N_{clusters} \rangle f}{\sigma_{pcc}} \tag{2.11}$$

Where σ_{pcc} is the visible cross section of the tracker with the PCC method and is determined through a Van der Meer scan (described in Chapter 3)

Vertex counting A second method for offline luminosity measurements using the tracker is with the reconstructed tracks, finding the primary interaction vertices and counting those. At low luminosity this is one of the cleanest measurements, as it also has no background. However, at high luminosity, collisions occur close to each other and become indistinguishable from tracks alone. Thus, this method is only used in calibration fills to help measure beam profiles more accurately.

2.3.7 The Drift Tubes

The drift tubes (Section 1.2) use the rate of muon track stubs. They do not provide per-bunch measurements and do not have the readout system necessary for Van der Meer calibration, however they have proven to be a very stable and linear luminosity measurement system that is used as an offline reference luminometer. It is cross-calibrated to another luminometer (HFET in 2017) in order to be used as a luminometer.

Chapter 3

Calibration of luminometers

3.1 Luminosity of Gaussian beams

It is usually assumed beam density distributions are factorizable and have Gaussian profiles in all directions. The beam density distribution for beam i becomes

$$\rho_i(x_i, y_i, z_i, \pm s_0) = \rho_{xi}(x)\rho_{yi}(y)\rho_{z_i}(z \pm s_0). \tag{3.1}$$

And so

$$\mathcal{L} = 2N_1N_2fN_b \iiiint \rho_{x1}(x)\rho_{y1}(y)\rho_{z1}(z+s_0)\rho_{x2}(x)\rho_{y2}(y)\rho_{z2}(z-s_0)\,\mathrm{d}x\,\mathrm{d}y\,\mathrm{d}z\,\mathrm{d}s_0\,, \tag{3.2}$$

where the factored terms are

$$\rho_{xi} = \frac{1}{\sigma_{xi}\sqrt{2\pi}}\exp\left[-\frac{(x-\mu_{xi})^2}{2\sigma_{xi}^2}\right], \tag{3.3}$$

$$\rho_{yi} = \frac{1}{\sigma_{y1}\sqrt{2\pi}}\exp\left[-\frac{(y-\mu_{yi})^2}{2\sigma_{yi}^2}\right], \tag{3.4}$$

$$\rho_{zi} = \frac{1}{\sigma_{z}\sqrt{2\pi}}\exp\left[-\frac{(z\pm s_0)^2}{2\sigma_{z}^2}\right], \tag{3.5}$$

where $\sigma_{xi,yi,z}$ are the corresponding beam widths and it is assumed the width in the z direction is the same. Equations 3.3-3.5 are Gaussian integrals, meaning

$$\int_{-\infty}^{\infty} e^{-x^2}\,\mathrm{d}x = \sqrt{\pi}. \tag{3.6}$$

Putting them into Equation 3.2 and integrating over z and s_0:

$$\mathcal{L} = \frac{2N_1N_2fN_b}{8\pi^2\sigma_{x1}\sigma_{x2}\sigma_{y1}\sigma_{y2}}\iint \exp\left[-\frac{(x-\mu_{x1})^2}{2\sigma_{x1}^2} - \frac{(x-\mu_{x2})^2}{2\sigma_{x2}^2}\right]\times \exp\left[-\frac{(y-\mu_{y1})^2}{2\sigma_{y1}^2} - \frac{(y-\mu_{y2})^2}{2\sigma_{y2}^2}\right]\mathrm{d}x\,\mathrm{d}y\,. \tag{3.7}$$

To evaluate the integral over x (equivalent to the one over y), a coordinate system where $\mu_{x1} = 0$ is chosen. Then $\mu_{x2} = d_x$ is the distance between the centers of the two beam distributions. The integral in question is then

$$\int_{-\infty}^{\infty} \frac{1}{2\pi\sigma_{x1}\sigma_{x2}} \exp\left[-\frac{x^2}{2\sigma_{x1}^2}\right] \exp\left[-\frac{(x-d_x)^2}{2\sigma_{x2}^2}\right] \mathrm{d}x\,. \tag{3.8}$$

This, as described in detail in Appendix A of [21], becomes

$$\begin{aligned} \frac{1}{2\pi\sigma_{x1}\sigma_{x2}} \exp\left[-\frac{d_x^2}{2(\sigma_{x1}^2+\sigma_{x2}^2)}\right] \int_{-\infty}^{\infty} \exp\left[-\frac{\sigma_{x1}^2+\sigma_{x2}^2}{2\sigma_{x1}\sigma_{x2}}\left(x-\frac{\sigma_{x1}^2 d_x}{\sigma_{x1}^2+\sigma_{x2}^2}\right)^2\right] \mathrm{d}x = \\ = \frac{1}{\sqrt{2\pi(\sigma_{x1}^2+\sigma_{x2}^2)}} \exp\left[-\frac{d_x^2}{2(\sigma_{x1}^2+\sigma_{x2}^2)}\right]. \end{aligned} \tag{3.9}$$

The last equality comes again from integrating a Gaussian function. Now the expression for luminosity becomes

$$\begin{aligned} \mathcal{L} = \frac{N_1 N_2 f N_b}{2\pi\sqrt{(\sigma_{x1}^2+\sigma_{x2}^2)(\sigma_{y1}^2+\sigma_{y2}^2)}} \exp\left[-\frac{d_x^2}{2(\sigma_{x1}^2+\sigma_{x2}^2)} - \frac{d_y^2}{2(\sigma_{y1}^2+\sigma_{y2}^2)}\right] = \\ = \frac{N_1 N_2 f N_b}{2\pi\sqrt{(\sigma_{x1}^2+\sigma_{x2}^2)(\sigma_{y1}^2+\sigma_{y2}^2)}}\mathcal{E}. \end{aligned} \tag{3.10}$$

Calibration at the LHC is done under special beam optics making the beam relatively larger, while keeping the beams well centered, rendering the exponent term in Equation 3.10 $\mathcal{E} \approx 1$, as shown in Table 3.1.

Table 3.1: Comparison of beam optics and filling scheme between calibration (Fill 6016) and a "normal" physics fill (fill 6362). Ranges in values account for bunch-to-bunch variations and differences in planes.

Conditions	Calibration	Physics
β^* [cm]	1917	30
$\alpha_{crossing}$ [µrad]	0	150
Colliding bunches	32	1866
Protons per bunch	9×10^{10}	12×10^{10}
Values here are illustrational:		
Beam width [µm]	80-90	12-14
Beam displacement (d_x) [µm]	0.3-2	0.5-1
$\mathcal{E}$	0.9999	0.998

Using this, the luminosity during a calibration fill of the LHC should be just

$$\mathcal{L} = \frac{N_1 N_2 f N_b}{2\pi\sqrt{(\sigma_{x1}^2+\sigma_{x2}^2)(\sigma_{y1}^2+\sigma_{y2}^2)}}. \tag{3.11}$$

As mentioned earlier, calibration of a luminometer consists of estimating its visible cross section. Putting Equation 3.11 into the connection between detector hit rates (R), detector visible cross section (σ_{vis}) and luminosity (Equation 2.3) the visible cross section can be expressed from beam parameters as

$$\sigma_{vis} = \frac{R}{\mathcal{L}} = \frac{2\pi R\sqrt{(\sigma_{x1}^2 + \sigma_{x2}^2)(\sigma_{y1}^2 + \sigma_{y2}^2)}}{N_1 N_2 f N_b}. \tag{3.12}$$

A commonly used expression for luminosity can be derived if the beams are also assumed to be the same size in the x and y directions ($\sigma_{x1} = \sigma_{x2} = \sigma_x$ and $\sigma_{y1} = \sigma_{y2} = \sigma_y$):

$$\mathcal{L} = \frac{N_1 N_2 f N_b}{4\pi\sigma_x\sigma_y}. \tag{3.13}$$

Then for the visible cross section:

$$\sigma_{vis} = \frac{R}{\mathcal{L}} = \frac{4\pi R\sigma_x\sigma_y}{N_1 N_2 f N_b}. \tag{3.14}$$

These are the general expressions most often used for calculating instantaneous luminosity from beam parameters.

3.2 Van der Meer method

The visible cross section is a parameter of the detector that, for an ideally linear luminometer, is independent of beam characteristics. Therefore it needs to be determined once every time the detector is installed and setup in a certain way. This is usually done once a year in a special fill using the so called Van der Meer scans, named after Simon van der Meer who first described it in 1968[22]. The method consists of moving or "scanning" the two beams across each other in each direction on the collision plane (x and y) in discrete steps of certain length, as illustrated in Figure 3.1. Measurements are averaged over each step.

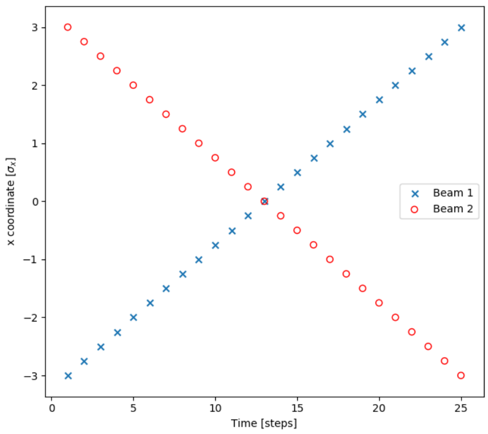

Figure 3.1: Visualization of the movement of the two beams during a Van der Meer scan in the x direction

According to Equation 3.10, assuming the beams are centered in one direction (y) while being scanned in the other (x), the resulting rate measurement averages R should follow a Gaussian distribution with width $\Sigma_x = \sqrt{\sigma_{x1}^2 + \sigma_{x2}^2}$, like so

$$R(d_x, d_y = 0) = \frac{\mathcal{L}}{\sigma_{vis}} = \frac{N_1 N_2 f N_b}{2\pi \Sigma_x \Sigma_y \sigma_{vis}} \exp\left[\frac{(d_x - \mu_x)^2}{2\Sigma_x}\right] = R_0 \exp\left[\frac{(d_x - \mu_x)^2}{2\Sigma_x}\right]. \quad (3.15)$$

Here $R_0 = R(d_x = 0, d_y = 0)$ is the peak rate in the detector and μ_x has been added to adjust for the beams not being perfectly centered when set to $d_x = 0$ by the LHC. Fitting this distribution in both the x and y directions with a Gaussian function gives the necessary parameters to calculate the visible cross section for the detector as

$$\sigma_{vis} = \frac{\pi(R_{0x} + R_{0y})\Sigma_x \Sigma_y}{N_1 N_2 f N_b}, \quad (3.16)$$

where the average of the two peak rate estimations R_{0x} and R_{0y} has been taken.

A constant term can be added to account for any background during calibration (background is generally insignificant in normal physics conditions). A sum of two Gaussian functions can also be used to provide a better fit as its variance is also the sum of the variances of the two Gaussians.

3.3 Corrections and uncertainties

There are a lot of assumptions made in the previous section and not all possible effects are considered. After the initial calibration outlined there, a multitude of studies are carried out to account for any possible discrepancies and each one of them yields a correction and/or an additional systematic uncertainty to the measurement. Although these investigations are not themselves the subject of this thesis, they are briefly outlined here for completeness. Detector-specific corrections are omitted. A more detailed account can be found in the 2017 CMS Luminosity Physics Analysis Summary (PAS)[23].

Length scale calibration

This accounts for the differences in actual beam separation from the desired separation set by the LHC magnets. To study these differences a set of special scans is conducted under calibration conditions and the primary vertices positions reconstructed by the CMS Tracker are used to determine the beam spot position. Two types of scans are used in CMS - one where the two beams are moved together while kept at a constant 1σ separation and one where a small 3-step scan is made with one beam across the other at multiple positions. A Gaussian function is used to fit each three points of the latter and its mean value is taken as the beam spot position. The measured beam spot positions are then linearly fitted against the nominal ones to determine the size of the correction and its uncertainty.

Orbit drift

Orbit drift is the potential movement of the LHC orbit during a VdM scan. CMS Beam Position Monitoring systems (BPM) are used to measure this position before, after and in the middle of each scan. The correction is applied to each half of a scan and is calculated as the linear fit between the two orbit position data points surrounding it.

The x-y correlations

This corrections aims to account for any non-factorizability of the beam density distributions in the xy plane. A pair of "imaging" scans are conducted in each direction, where one beam is scanned across, while the other is stationary. This allows the measurement of the stationary beam's particle density distribution. A more complex model including a third, negative Gaussian added to the double Gaussian function is used to fit the data. The correction is derived through multiple Monte Carlo simulations of a VdM scan using the measured beam densities.

Beam-Beam effects

Two effects caused by beam-beam interactions are corrected for.
The first is the lateral electric deflection between the two beams that affects their separation. It is calculated as described in [24] and needs a Σ measurement input that means every scan needs to be fitted twice - before and after this correction. This is one of the largest corrections as it is usually at the percent level and is applied to almost any VdM-like analysis.
The second effect is called dynamic-β effect and account for the defocusing of the two beams by each other. It is a correction applied to the rates and determined through beam transport simulations[25].

Bunch current normalization

Two possible corrections are accounted for in the bunch current measurement. The first is from the normalization of the Fast Beam Current Transformers (FBCT) per-bunch beam current measurements (whose relative uncertainty is negligible) to the

DC current transformers (DCCT) that measure all of the charge in the LHC accurately[26].
The second is the "satellite" and "ghost" charges correction. The former are charges that are in the colliding bunch slot, but not in the correct RF bucket, while the latter are outside of any filled bunch slot. They are measured by the DCCT but they do not contribute to measured luminosity.

Linearity and stability

The ideal detector has a completely linear, constant and reliable response to luminosity. Of course, real-world luminometers have various issues with both, and even after correcting each individual detector, some discrepancies are still evident. A systematic uncertainty is taken to account for these from comparisons between each pair of detectors. A new approach using short VdM-like scans in each fill has been used to correct for such effects and reduce the systematic uncertainty and will be discussed further in Chapter 5.

Chapter 4

Van der Meer scan analysis framework

Van der Meer scan analysis in the CMS collaboration is conducted using a software framework written in Python 2 and utilizing CERN's data analysis package ROOT[27] via the PyRoot[28] library. The framework was first developed for Run II of the LHC (starting 2015) as a centralized software package for the Van der Meer (VdM) analysis for CMS luminometers.

The framework takes data from BRIL DAQ and from the LHC through the Data Interchange Protocol (DIP)[29], does some data manipulation, applies some corrections, fits one of several predefined Gaussian-like functions to the data and uses the resulting $\Sigma_{x,y}$ and $P_{x,y}$ to calculate the calibration constant for the detector via Equation 3.16. Multiple data and visualization files are made in the process to allow further analysis and tests: average rates per step, average beam intensities per step, various corrections applied, fitted graphs, etc.

The framework was largely unchanged until 2017, when the amount of data to be analysed was vastly increased - from several dozens of fits for 3-4 detectors once a year, to a more or less daily run of several thousand fits for > 50 detector channels - warranted a major overhaul of the system. Backwards compatibility has been kept as much as possible by implementing a wrapper of sorts to the already developed framework, but large parts of it had to be redone to comply with new requirements. Both the old[30, 31] and the new[32, 33] versions of the framework, as well as some simple documentation[34, 35] are available online.

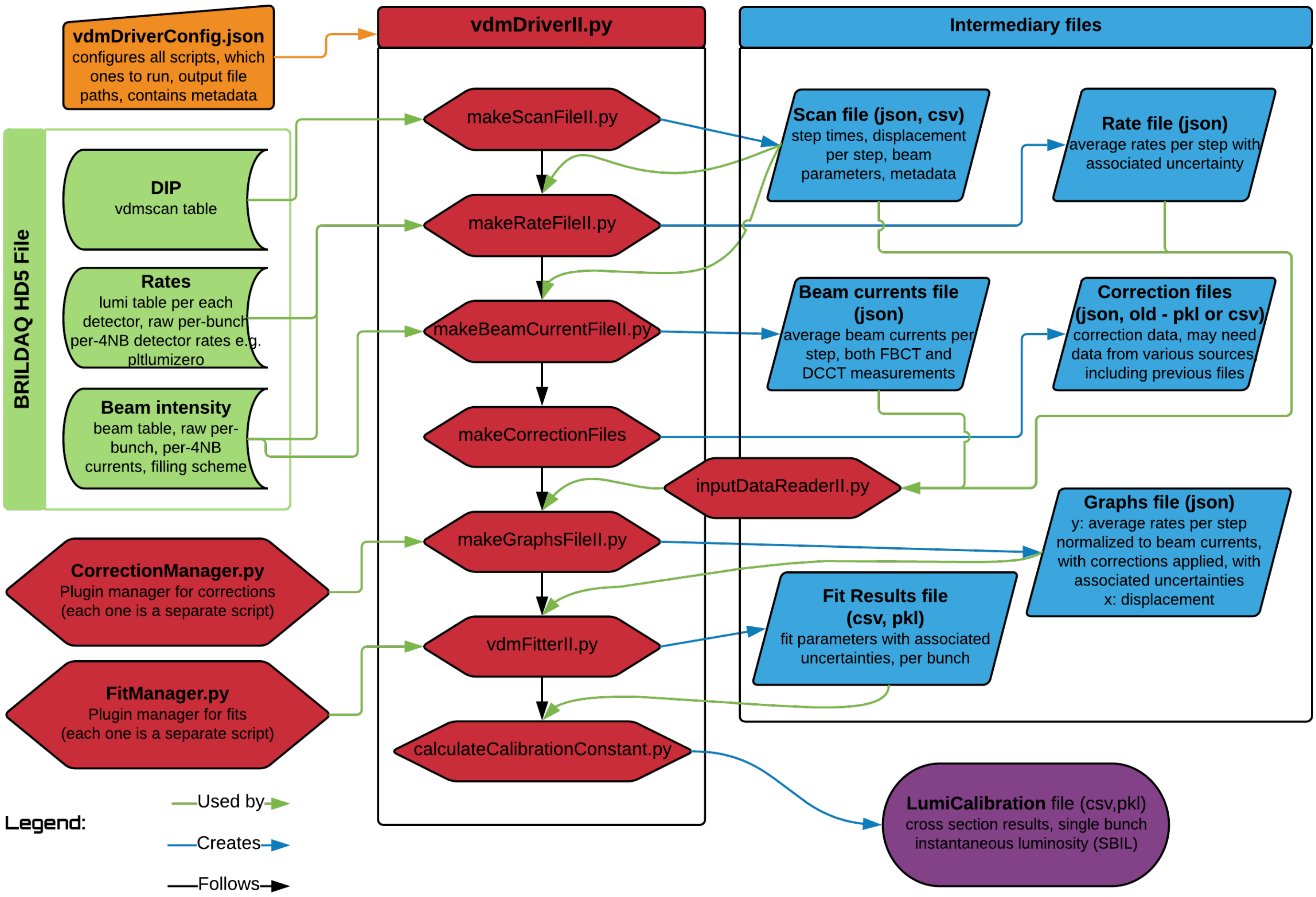

Figure 4.1: Van der Meer Analysis Framework Core Diagram (log and visualization files not mentioned)

This chapter aims to document the inner workings and usage of both the updated "core" framework (as well as changes compared to original) and its "automation wrapper".

4.1 Core framework

The core framework (visualized in Figure 4.1) is ran using a large JSON[36] configuration file (see example at section A.1) for the main script, **vdmDriverII.py**, which in turn runs all other scripts. The configuration file contains multiple separable configurations for each script which could be ran completely separately. This generally requires some human input, like timestamps for beginnings and endings of scans, folder structure, file names, fit function choice, etc. The basic process for the framework is:

1. **Make scan file** - Get DIP data (step start and end timestamps, separations between beams, crossing angle, β^*, etc) either from BRIL DAQ data dumps(HDF5[37] files) or from the separate DIP data dump file (csv), format them properly and save to a csv (human-readable) and a json (easily computer readable).

2. **Make rate file**

   (a) Get BRIL DAQ luminometer data - per bunch raw rates integrated over four "lumi-nibbles" (NB4). A nibble is equal to 4096 (2^{12}) LHC orbits or around 364 ms.

   (b) Get BRIL DAQ beam data to determine the filling scheme (the colliding bunch numbers whose rates need to be saved). This is done using a threshold (currently 6×10^9 protons per bunch) as sometimes there are low intensity bunches used for machine diagnostics that should not be included in averages.

   (c) Take step start and end timestamps from scan file.

   (d) Average the per-NB4 measurements over each step for each colliding bunch and calculate associated uncertainties. This used to be done as a standard error on the mean of the measurements, but in 2018 this was determined to often underestimate the uncertainty and a binomial error is now calculated for zero-counting algorithms.

3. **Make beam currents file**

   (a) Get BRIL DAQ beam data and scan file.

   (b) Average per-NB4, per-BX measurements of each beam intensity over each step. Uncertainty is assumed to be negligible.

4. **Make correction files** - Corrections applied trough the framework are generally separated into two scripts - one that makes a data file outlining the correction and a second that reads that file and applies it during the graph-making process.

5. **Make graph file**

   (a) Load **Input data reader** script to load the scan, rate and beam currents files. The input data reader loads all the data into memory multiple times with different ways of accessing it (by step, by bunch, etc.).

(b) Load **Correction Manager** - a plugin manager for the different correction scripts - and apply corrections. Currently supported corrections by the framework are:

   i. **Beam-Beam correction**, accounting for lateral electric deflection of the beams, changing the real beam separation;

   ii. **Length scale correction**, accounting for differences between the nominal beam separation set by the LHC magnets and the actual separation;

   iii. **Ghost and satellite charges corrections** - satellite charges are charges in the colliding bunch but not the colliding RF bucket, ghost charges are charges outside of any nominally filled bunch slots;

   iv. **Background correction** - first used for 2017 calibration, this correction estimates noise and beam induced background from the abort gap and from filled non-colliding bunches, respectively, thus removing a constant term from the fit function.

(c) **Normalize rates** - divide each rate measurement by the corresponding beam currents and multiply by 10^{22} (the latter is just for readability).

(d) Save resulting normalized rates and corresponding separation values to a new "graphs" file, each BX is a separate graph.

6. **Fit** Load another plugin manager called "Fit Manager" which loads different fit scripts (most commonly a single Gaussian (SG), a double Gaussian (DG) and either of those plus a constant). Each fit script creates a ROOT TF1 function and fits each graph to such a function using Minuit. The resulting fit parameters are saved to a csv table. Optionally a visualization of each "shape" (set of points) and its fit is made and saved to a PDF file. Figure 4.2 shows a scan pair example for a single bunch from the 2017 VdM scan program calibrating the PLT.

7. **Calculate visible cross section** Get the resulting Gaussian parameters (peak rates, Σ) from the X and Y scan and use them to calculate the calibration constant using Equation 3.16.

Every step is optional and can be set through the configuration file. For the scan, rates and beam currents files the default setting is "False", and they get automatically made if they are not already available. This is done to simplify the automation process.

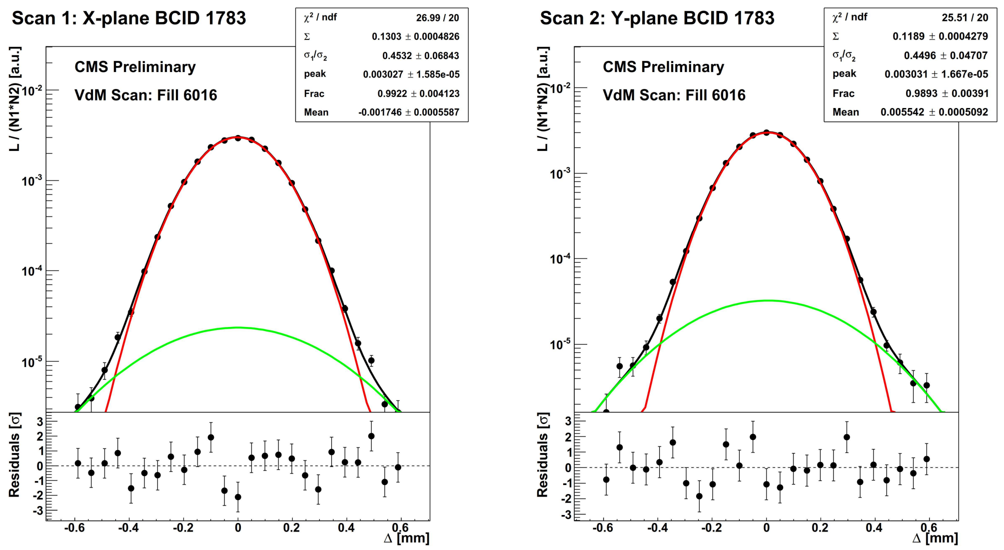

Figure 4.2: Normalized rates and the resulting fitted double Gaussian scan curves as a function of the beam separation (Δ) for a single bunch as recorded by PLT for a scan in the x (left) and y direction (right). Background subtraction has been applied to the raw data. Beam-beam deflection and Length scale corrections have been applied.

4.2 Automation wrapper

As mentioned in the previous chapter, in 2017 the amount of data that needed to be analysed vastly increased. It used to be an (ideally) once per year calibration of 4-5 luminometers from several scans with 32 colliding bunches, which made the manual configuration, single thread, intermediary data output in multiple format of the core VdM framework a viable option. In 2017 there was a need to start analyzing so-called "emittance scans" for various stability and linearity studies. Emittance scans are short (7-9 steps of 10 seconds each, compared to 25 30-second-steps for the normal VdM scan) VdM-like scans conducted at the beginning and planned dump of each LHC Fill. Additionally, a new readout system in operation for BCM1F as well as the need for per-channel analysis of both BCM1F and PLT increased the number of analysed detectors over 20 times. Results from analysis also needed to be sent to a web page for monitoring purposes.

This required a new automated, threaded and optimized approach for the VdM framework. Backwards compatibility was kept as much as possible and so the automation was done through several new scrips that acted as a wrapper of sorts to the VdM Driver script (the core framework). File naming is self-resolved and all files are saved and looked for in configurable "Automation" folder (not necessarily named "Automation").

4.2.1 The Configurator script

This is the script that automates all the manual input of DIP-related and metadata to the VdMDriver configuration (section A.1). Step by step, it:

1. Gets the DIP data from the hd5 file and converts it to a csv file of the old format used by the core framework;
2. Finds where scans begin and end (previously done by hand);
3. Loads template configurations (json configurations like section A.1 with various parts removed and replaced with keywords);
4. Uses all that to make configurations for the VdMDriver script and save them to `{Automation folder}/autoconfigs/{scanname}/` under the format `{luminometer}_{corr1_corr2_etc}_{fit}_driver.json`;
5. Makes a second configuration if the Beam-Beam correction is included one without the correction to get a Σ measurement that is a necessary input for the Beam-Beam correction.

4.2.2 The RunAnalysis script

1. Finds pre-made (either by hand or by configurator) configurations according to the naming convention described in the previous paragraph;
2. Calls VdMDriver with those configurations, automatically running twice with different configurations if the Beam-Beam correction is included;
3. Does error handling and logging;
4. Loads the FitResults and LumiCalibration files into Pandas[38] data frames and returns them.

This script can (or perhaps should) be made part of the VdMDriver script in the future.

4.2.3 The PostVdM script

As already mentioned, results from analysis needed to be uploaded to a database and shown on a web page for monitoring purposes. The script:

1. Takes FitResults and LumiCalibration Pandas data frames and extracts Σ, R_{peak}, μ, χ^2, σ_{vis} and SBIL;

2. Calculates averages over all bunch crossings for each variable;

3. Fits σ_{vis} against SBIL as a linear function for lead (first in train) and train bunches;

4. Puts all this data plus some metadata into a JSON file and saves it to the main folder of the scan;

5. Optionally publishes to one of three web service endpoints (main, test and per-channel) which then save the data to a database that is the source for web monitor pages;

6. Determines channel number (if analysed data is from a single channel) from luminometer name using regular expression `([A-Z1_]*[A-Z]+)_?([0-9]+)`.

4.2.4 The AutoAnalysis script

This script is the main entry point when using the automation wrapper of the framework. It can analyse a single HD5 file, a pair of them (in case two scans of an XY pair are separated accidentally) or it can check a folder periodically and analyse single HD5 files as they arrive ("watcher" mode). It also uses a JSON configuration file (see section A.2) that sets:

- folder paths (Automation folder, logs folder, data source folder;

- the minimum number of steps in a scan to use a double Gaussian function;

- the number of seconds to wait before checking the data source folder when in watcher mode;

- the maximum number of threads the script is allowed to use at the same time;

- the names of the tables in the HD5 files (ratetables) of "main" luminometers that should be posted to main web monitoring page.

The rest of the options are done through command line arguments as follows:

- `-f {hd5 file path}` When a single file needs to be analysed outside of the watcher loop;
- `-c {folder path}` Data source folder, in case different from configuration file;
- `-b` Apply Beam-Beam correction;
- `-t` Only analyse the luminometers from the config file;
- `-p` Post one-time analysis to web monitoring (watcher automatically posts);
- `-f2 {hd5 file path}` Second scan of the scan pair (if scan pair is split);
- `-d` Force double Gaussians instead of single;
- `-pdf` Make PDF files with visualizations of Beam-Beam correction and fitted functions;
- `-l` Make logs for the fitting (both fit function scripts and Minuit logs);
- `-ls` Apply length scale correction (only applicable if you have length scale data);
- `-bg` Apply background correction.

Once the path to an HD5 file (or two) is received, the script:

1. Creates the Automation folder at the specified path if it does not exist, as well as 3 folders inside it - **Analysed_Data, autoconfigs** and **dipfiles**.
2. Loads DIP data from the **vdmscan** table in the table and uses the remapping function from the Configurator script and saves the result to the dipfiles folder.
3. Gets the timestamps of starts and ends of scans using the Configurator script and treats them as XY scan pairs from there on out.
4. Finds all luminosity tables in the HD5 file by their names using the regular expression `(.*)_?lumi[a-z]*_?(.*)` where the capitalized version of the first group is then considered the name of the luminometer and the second part should contain a channel number and algorithm tag in the case of BCM1F.
5. Decides on whether to use a double or a single Gaussian fit depending on he number of steps and whether the `-dg` option was used.

6. Names each scan as `{Fill}_{startdate&time}_{enddate&time}`. Folders with this name are created in autoconfigs and Analysed_Data folders.

7. Calls runAnalysis script once over a single luminometer to get the common files (scan file, beam currents file, etc) created using the subprocess[39] library and the Popen function.

8. Runs the rest of the found luminometers in batches of 10 unless the `-t` option was used, in which case only the ones from the configuration file get analysed. The maximum number of simultaneous runs is configurable in the AutoAnalysis JSON configuration file (Appendix A.2).

9. At the end of each batch calls the PostVdM script on the finished luminometers. By default, in watcher mode everything gets published to the web monitoring, and if the `-p` option was invoked when analysing a single file.

10. Gives full access rights on all files created to all users (since this is done within a completely separated cluster).

Chapter 5

Emittance scans for CMS luminosity calibrations

In 2015 the LHC started conducting small Van-der-Meer-like scans just after declaring stable beams (”early scan”) and before any planned beam dump (”late scan”) each fill . Figure 5.1 shows the luminosity during a fill, the emittance scans are visible as short dips at the beginning and at the end of the fill. Each scan had 7 steps of 10 seconds and reached a maximum separation of $\pm 3\sigma$. The purpose of these scans was to derive plane-by-plane, bunch-by-bunch emittances and orbit offsets using CMS luminosity measurements, which is why they are now called ”emittance scans”[40, 41].

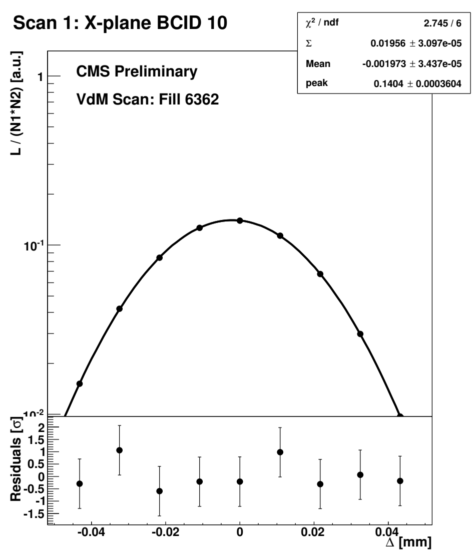

Figure 5.2: Example of a single Gaussian fit to an emittance scan in Fill 6362

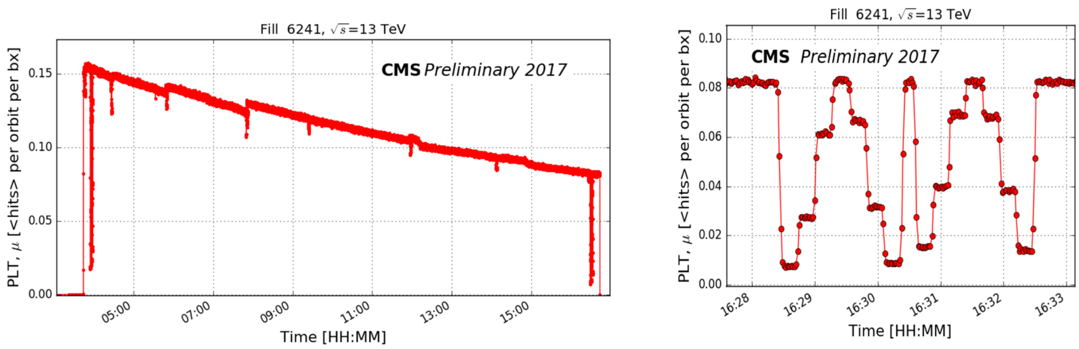

Figure 5.1: μ values for the PLT during the whole fill 6241 (left) and a zoom-in on the late emittance scan(right)

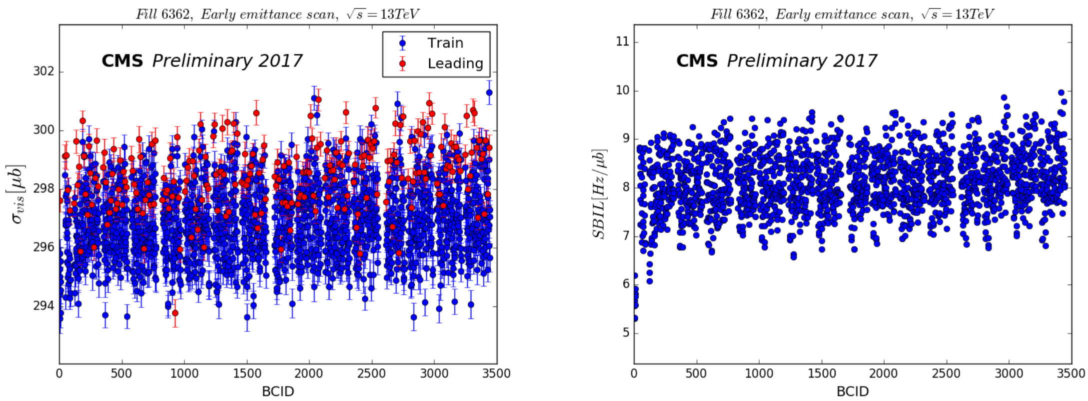

Figure 5.3: Per-BX σ_{vis} (left) and SBIL (right) measurements by the PLT from the early scan in LHC Fill 6362

In 2017 data from emittance scans were analysed similarly to data from calibration VdM scans and the results were used for stability and linearity studies of the CMS luminosity detectors. During the year the number of steps in a scan was increased to 9 to allow for a better beam shape measurement. Figure 5.2 shows an example of the fits to such data, with a zoom-in on a late scan on the right. Each point on the plot is an average of the measurements made during the step (5-6 measurements each).

5.1 Non-linearity of a luminometer's response

The system setup by BRIL using the automated framework described in Chapter 4 outputs per-bunch-crossing (per-BX) measurements of the visible cross section and single bunch instantaneous luminosity (SBIL). Figure 5.3 shows such measurements for the PLT detector. It is important to note the difference between leading (first in train) and the rest of the bunches in a train, as well as the large range of SBIL across the bunch crossings in a single fill - between 6 and 10 $Hz/\mu b$ during early scans and between 2 and 4 $Hz/\mu b$ during late ones, depending on the duration of the fill.

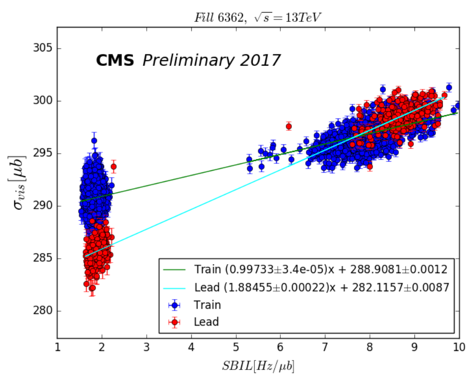

Figure 5.4: PLT σ_{vis} as a function of SBIL in Fill 6362, both scans

This large range allows for studies of the dependence of σ_{vis} on SBIL, which should be a constant for an ideal luminometer. As seen in Figure 5.4, that is not the case - in fact two separate linear dependencies can be determined for the leading and train bunches. The dependency is more pronounced in the early scan (the group of points at high SBIL on the plot) but can be traced down to the

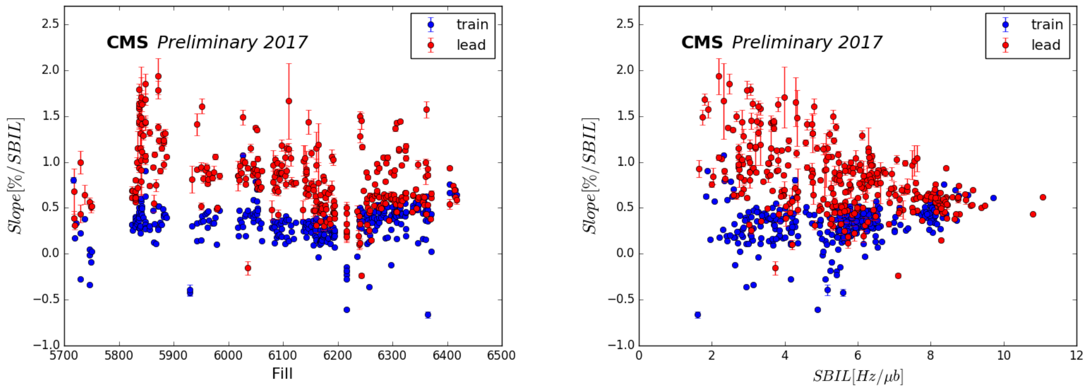

Figure 5.5: Per-scan slope of PLT $\sigma_{vis}(SBIL)$ as a function of LHC Fill number (left) and SBIL (right)

results from the late scan (low SBIL points on the plot). A study of this dependency has been conducted on a per-scan basis. Figure 5.5 shows the calculated slope in each scan as a function of Fill number (left) and as a function of the average SBIL calculated in that scan (right). It is noticeable that the effect is generally larger on leading bunches, but the difference grows smaller at higher SBIL.

A separate measurement can be made by fitting average σ_{vis} as a function of average SBIL per scan. As shown in Figure 5.6, the results agree well between the two methods.

A data-driven simulation was carried out that showed a linear dependence between the linear term in $\sigma_{vis}(SBIL)$ and the nonlinear (quadratic) term in the detector's response function, with the ratio between the two terms in the range of $\approx 0.3 - 0.7$. Further studies need to be done to be conducted for a better estimate of this parameter. However, it is important to note this gives a new method for estimating the non-linearity in a detector's response and that it is self-contained, as it does not rely on comparison to other detectors.

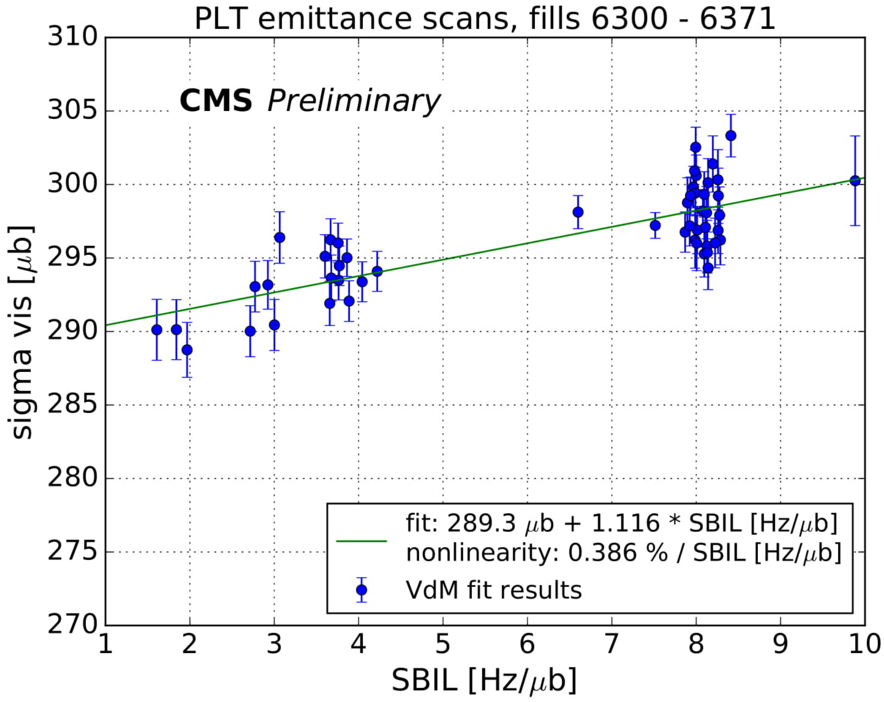

Figure 5.6: PLT σ_{vis}(SBIL) in Fills 6300-6371. This is a stable period for the PLT

5.2 Luminometer stability

It has already been established that emittance scans cross section and SBIL measurements are strongly affected by detector response quality. It is therefore not surprising they can be used for stability monitoring. Figure 5.7 shows how average σ_{vis} per scan can reveal long term stability problems - the highlighted areas were periods where the PLT was losing efficiency. The problem was fixed by raising the operational high voltage. As described in Chapter 4, all emittance scans are automatically analysed and the results are published to a database and displayed on web monitoring pages to help shifters notice long term issues quicker. For the offline luminosity measurement a stability correction was derived from the average cross section for each fill.

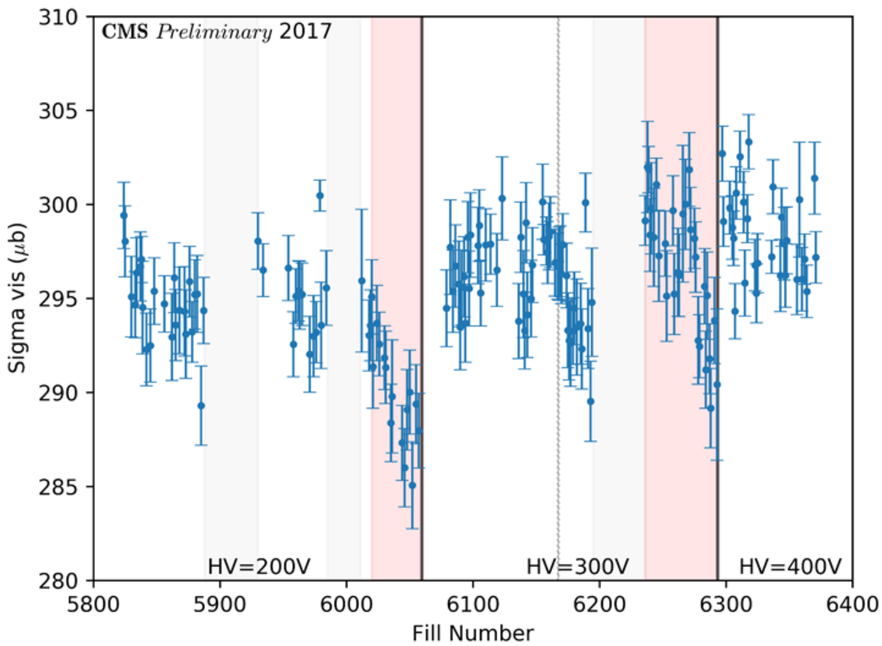

Figure 5.7: Average PLT visible cross section per fill for all data from 2017. Error bars signify standard deviation of the per BX measurements in the average. Regions of loss of efficiency are highlighted.

Conclusion

Luminosity measurements are vital to any high energy physics experiment. They go into any results coming out of the experiment and are still one of the largest contributors to the systematic uncertainty of the various physics cross section measurements.

One of the biggest uncertainties in luminosity comes from non-linearities - it is estimated through the ratio of integrated luminosity measurements of multiple detectors and as none of them is an ideal luminometer uncertainties stack up. In 2017 a new self-contained (reliant only on a single luminometer's data) method for non-linearity estimation (and correction) has been devised by the CMS collaboration in an effort to mitigate this effect.

The new method is based on analysing short Van-der-Meer-like scans ("emittance" scans) at the beginning and end of each LHC fill. It has been determined that the resulting visible cross section measurements depend linearly on the single bunch instantaneous luminosity (SBIL). The linearity coefficient has been found to be proportional to the non-linear (quadratic) term of the detector's response function.

The technique vastly increased the amount of data needed to be analysed. The software framework used by the CMS collaboration for Van der Meer scan analysis needed to be reworked to accommodate this change. Data output and various other processes were optimized, configuration and analysis for each scan was automated based on incoming data. Ability to analyse multiple detector's data in parallel was added to provide quick feedback from analysis.

Emittance scans visible cross section results can also be used to monitor luminometer efficiency and long term stability. Results from the analysis (various fit parameters, visible cross section, SBIL, etc.) are automatically sent to a web monitoring page.

The extended automated Van der Meer analysis framework became a valuable asset for luminosity measurements at CMS in 2017 and it is still used and becoming exceedingly important to the BRIL project and the CMS experiment in general.

Appendix A

VdM Framework JSON configuration files

A.1 Example VdMDriver Configuration

```
{
  "Fill": "6016",
  "Date": "28Jul2017",
  "Luminometer": "PLT",
  "AnalysisDir": "Fill6016Final/Analysed_Data/6016_28Jul17_115005_28Jul17_121320",
  "CorrLater" : ["noCorr", "LengthScale", "Ghosts", "Satellites", "BeamBeam","Background"],
  "Corr" : ["BeamBeam", "LengthScale", "Background"],
  "Comment": "Output of following step goes to <AnalysisDir>/cond",
  "makeScanFile": false,
  "Comment": "Output of following step goes to <AnalysisDir>/LuminometerData",
  "makeRateFile": false,
  "Comment": "Output of following step goes to <AnalysisDir>/cond",
  "makeBeamCurrentFile": false,
  "Comment": "Output of following step goes to <AnalysisDir>/corr",
  "makeBeamBeamFile": true,
  "Comment": "Output of following step goes to <AnalysisDir>/corr",
  "makeGhostsFile": false,
  "Comment": "Output of following step goes to <AnalysisDir>/corr",
  "makeSatellitesFile": false,
  "Comment": "Output of following step goes to <AnalysisDir>/corr",
  "makeLengthScaleFile": true,
  "Comment": "Output of following step goes to <AnalysisDir>/corr",
  "makeBackgroundFile": true,
  "Comment": "Output of following step goes to <AnalysisDir>/<Luminometer>/graphs",
  "makeGraphsFile": true,
  "Comment": "Output of following step goes to <AnalysisDir>/<Luminometer>/graphs",
  "makeGraphs2D": false,
  "Comment": "Output of following step goes to <AnalysisDir>/<Luminometer>/results/<Corr>",
  "runVdmFitter": true,
  "Comment": "Output of following step goes to <AnalysisDir>/<Luminometer>/results/<Corr>",
  "calculateCalibrationConstant": true,
  "MakePDF": true,
  "MakeLogs": false,
  "makeScanFileConfig":
      {
      "InputCentralPath":
      ↪  "/eos/cms/store/group/dpg_bril/comm_bril/vdmdata2017/6016_1707280946_1707281036.hd5",
      "InputDIPFile" : "Fill6016Final/dipfiles/dip_6016_28Jul17_114757_28Jul17_123125.csv",
          "ScanNames" : ["X1", "Y1"],
          "Comment" : "Since X,Y scans are automatically differentiated, a time window can
          ↪  include an X and a Y scan, will still work, timestamp in UTC",
```

```
            "ScanTimeWindows" : [[1501235405, 1501236476], [1501236800, 1501237885]],
        "Comment" : "A few parameters that are not in our current DIP file, but should be available eventually",
        "Comment" : "betaStar in m, angle in microrad",
        "BetaStar" : 19.17,
        "Angle" : 0,
        "Offset" : [0.0, 0.0],
        "ParticleTypeB1" : "proton",
        "ParticleTypeB2" : "proton",
        "Comment": "Beam energies in MeV",
        "EnergyB1" : 6500,
        "EnergyB2" : 6500,
        "OutputSubDir" : "cond"
        },
    "makeRateFileConfig":
        {
        "Comment": "The following directories are relative to <AnalysisDir>",
        "InputScanFile": "cond/Scan_6016.json",
        "InputLumiDir" : "/eos/cms/store/group/dpg_bril/comm_bril/vdmdata2017/6016_1707280946_1707281036.hd5",
        "RateTable": "pltlumizero",
        "OutputSubDir": "LuminometerData"
        },
    "makeBeamCurrentFileConfig":
        {
        "InputCentralPath": "/eos/cms/store/group/dpg_bril/comm_bril/vdmdata2017/6016_1707280946_1707281036.hd5",
        "Comment": "Input scan file in <AnalysisDir>/<InputScanFile>",
        "InputScanFile" : "cond/Scan_6016.json",
        "OutputSubDir" : "cond",
        "CalibrateFBCTtoDCCT" : false
        },
    "makeBeamBeamFileConfig":
        {
        "Comment": "Input scan info file is <AnalysisDir>/<InputScanFile>",
        "InputScanFile" : "cond/Scan_6016.json",
        "Comment": "Input beam currents file is <AnalysisDir>/<InputBeamCurrentFile>",
        "InputBeamCurrentFile" : "cond/BeamCurrents_6016.json",
        "Comment": "Input luminometer data in <AnalysisDir>/<InputLuminometerData>",
        "InputLuminometerData" : "LuminometerData/Rates_PLT_6016.json",
        "Comment": "Input CapSigmas in <AnalysisDir>/<Luminometer>/results",
        "InputCapSigmaFile" : "Background/DG_FitResults.pkl",
        "Scanpairs" : [[1, 2]],
        "Comment": "This is relative to <AnalysisDir>",
        "OutputSubDir": "corr"
        },
    "makeGhostsFileConfig":
        {
        "Comment" : "Where to find the correction factors in json format",
        "InputDataDir" : "dataPrep_corr/corrData",
        "Comment": "This is relative to <AnalysisDir>",
        "OutputSubDir": "corr"
        },
    "makeSatellitesFileConfig":
        {
        "Comment" : "Where to find the correction factors in json format",
        "InputDataDir" : "dataPrep_corr/corrData",
        "Comment": "This is relative to <AnalysisDir>",
        "OutputSubDir": "corr"
        },
    "makeLengthScaleFileConfig":
        {
        "Comment": "Length scale scan fill",
        "FillLS": "6016",
        "Comment" : "Where to find the correction factors in json format",
        "InputDataDir" : "dataPrep_corr/corrData",
        "Comment": "This is relative to <AnalysisDir>",
        "OutputSubDir": "corr"
```

```
        },
    "makeGraphsFileConfig":
        {
        "Comment": "Input scan file in <AnalysisDir>/<InputScanFile>",
        "InputScanFile" : "cond/Scan_6016.json",
        "Comment": "Input beam currents file in <AnalysisDir>/<InputBeamCurrentFile>",
        "InputBeamCurrentFile" : "cond/BeamCurrents_6016.json",
        "Comment": "Input luminometer data in <AnalysisDir>/<InputLuminometerData>",
        "InputLuminometerData" : "LuminometerData/Rates_PLT_6016.json",
        "OutputSubDir" : "graphs",
        "MakePDF": true
        },
    "makeGraphs2DConfig":
        {
        "Comment": "Defines each X/Y pair for which to make 2D graphs",
        "Scanpairs" : [[1, 2]],
        "Comment": "Input/output directory is <AnalysisDir>/<Luminometer>/graphs",
        "InOutSubDir": "graphs"
        },
    "vdmFitterConfig":
        {
        "Comment": "Input graphs file in <AnalysisDir>/<Luminometer>/graphs",
        "InputGraphsFile" : "graphs/graphs_6016_BeamBeam_LengthScale_Background.json",
        "FitName" : "DG",
        "FitConfigFile" : "fits/DG_Config.json",
        "ScanNames" : ["X1", "Y1"],
        "MinuitFile" : "DG_BeamBeam_LengthScale_Background_Minuit"
        },
    "calculateCalibrationConstantConfig":
        {
        "Fill" : "6016",
        "AnalysisDir" : "Fill6016Final/Analysed_Data/6016_28Jul17_115005_28Jul17_121320",
        "Luminometer": "PLT",
        "Corr" : ["BeamBeam", "LengthScale", "Background"],
        "Comment": "Input fit results file in <AnalysisDir>/<Luminometer>/results/<Corr>",
        "InputFitResultsFile" : "DG_FitResults.pkl",
        "LuminometerSettings":
            {
            "LuminometerName": "PLT",
            "Comment": "defaults to settings in luminometer.py",
            "Comment": "needs to be set for non-default settings or for new luminometer",
            "LuminometerDescription": "default",
            "WhatIsMeasured": "default",
            "NormalizationGraphs": "default",
            "OldNormAvailable": "false"
            },
        "Comment": "Total inelastic cross section in microbarn, for pp at 8TeV",
        "Total_inel_Xsec": 72700,
        "Comment": "Use negative number to make clear that no old normalization is available",
        "Comment": "For low energy pp: 10.2; for pp at 8TeV, as determined in April 2012 scan:
        ↪  6.36",
        "Comment": "For pPb, as determined in Sep 2012 pilot run, taking into account that Pb ion
        ↪  is stripped of all its 82 electrons: 6.36/115.8*82",
        "OldNormalization": 10.2,
        "FormulaToUse": "1D-Gaussian-like",
        "Scanpairs" : [[1, 2]]
        }
}
```

A.2 Example AutoAnalysis JSON configuration

```
{
  {
```

```
      "Comment": "Results folder, watch folder, max threads to use, steps needed for double Gaussian, ratetables to analyse",
      "automation_folder": "Automation/",
      "central_default": "/brildata/vdmdata18/",
      "log_folder": "Automation/",
      "max_threads": 10,
      "dg_steps": 10,
      "ratetables": [
        "pltlumizero",
        "hfetlumi",
        "hfoclumi",
        "bcm1fsilumi",
        "bcm1fpcvdlumi",
        "bcm1fscvdlumi",
        "bcm1futca_pcvdlumi_100",
        "bcm1futca_pcvdlumi_101",
        "bcm1futca_silumi_100",
        "bcm1futca_silumi_101"
      ]
    }
  }
```

References

[1]L. Evans and P. Bryant, Lhc machine, Journal of Instrumentation **3**, S08001 (2008).

[3]CERN, Design concept for a 100 GeV e+e- storage ring (LEP), CERN Yellow Reports: Monographs (1977).

[4]*Buckets and bunches*, https://www.lhc-closer.es/taking_a_closer_look_at_lhc/0.buckets_and_bunches (visited on 06/15/2018).

[5]*Lhc running*, https://www.lhc-closer.es/taking_a_closer_look_at_lhc/0.lhc_running (visited on 06/15/2018).

[6]A. M. Sirunyan et al., Measurement of prompt and nonprompt charmonium suppression in PbPb collisions at 5.02 TeV, Eur. Phys. J. **C78**, 509 (2018).

[7]by Michaela Schaumann for the LHC team and C. Pralavorio, LHC report: xenon in action, (2017).

[8]C. Collaboration, Observation of a new boson at a mass of 125 GeV with the CMS experiment at the LHC, Physics Letters B **716**, 30–61 (2012).

[9]A. Collaboration, Observation of a new particle in the search for the Standard Model Higgs boson with the ATLAS detector at the LHC, Physics Letters B **716**, 1–29 (2012).

[10]T. C. Collaboration, The cms experiment at the cern lhc, Journal of Instrumentation **3**, S08004 (2008).

[11]W. C. Middelkoop and A. Schoch, Interaction rate in colliding beam systems, tech. rep. CERN-AR-Int-SG-63-40 (CERN, Geneva, 1963).

[12]C. Møller, *General Properties of the Characteristic Matrix in the Theory of Elementary Particles*, Vol. 23.1, Matematisk-Fysiske Meddelelser, Vol. 23, No. 1 1 (1945).

[14]M. Guthoff, Instrumentation for beam radiation and luminosity measurement in the CMS experiment using novel detector technologies, Nucl. Instrum. Meth. **A845**, 565–569 (2017).

[15]G. B. et al., The cms data acquisition system software, Journal of Physics: Conference Series **219**, 022011 (2010).

[16]P. Lujan on behalf of the CMS Collaboration, Performance of the pixel luminosity telescope for luminosity measurement at cms during run2, in, Vol. 314, doi:https://doi.org/10.22323/1.314.0504 (Mar. 2018).

[18] A. Bell, E. Castro, R. Hall-Wilton, W. Lange, W. Lohmann, A. Macpherson, M. Ohlerich, N. Rodriguez, V. Ryjov, R. S. Schmidt, and R. L. Stone, Fast beam conditions monitor BCM1F for the CMS experiment, Nuclear Instruments and Methods in Physics Research A **614**, 433–438 (2010).

[19] Absolute Calibration of the Luminosity Measurement at CMS: Winter 2012 Update, tech. rep. CMS-PAS-SMP-12-008 (CERN, Geneva, 2012).

[20] CMS Luminosity Based on Pixel Cluster Counting - Summer 2012 Update, tech. rep. CMS-PAS-LUM-12-001 (CERN, Geneva, 2012).

[21] P. Castro, Luminosity and beta function measurement at the electron-positron collider ring LEP, Presented on 25 Nov 1996 (1996).

[22] S. van der Meer, Calibration of the effective beam height in the ISR, tech. rep. CERN-ISR-PO-68-31. ISR-PO-68-31 (CERN, Geneva, 1968).

[23] CMS luminosity measurement for the 2017 data-taking period at $\sqrt{s} = 13$ TeV, tech. rep. CMS-PAS-LUM-17-004 (CERN, Geneva, 2018).

[24] M. Bassetti and G. A. Erskine, Closed expression for the electrical field of a two-dimensional Gaussian charge, tech. rep. CERN-ISR-TH-80-06. ISR-TH-80-06 (CERN, Geneva, 1980).

[25] A. Babaev, Beam-dynamic effects at the cms bril van der meer scans, Journal of Instrumentation **13**, C03028 (2018).

[26] G. Anders, N. Bacchetta, V. Balagura, C. Barschel, D. Belohrad, D. Berge, H. Burkhardt, S. I. Cooper, M. Ferro-Luzzi, G. Franzoni, C. Gabaldon, M. Gagliardi, J. J. Gras, V. Halyo, B. Heinemann, P. Hopchev, A. Hunt, W. Kozanecki, S. Kwan, M. Ludwig, D. Marlow, P. Odier, S. Pagan Griso, J. Panman, T. Pauly, S. Thoulet, S. White, J. C. Yun, and M. Zanetti, LHC Bunch Current Normalisation for the April-May 2010 Luminosity Calibration Measurements, (2011).

[27] R. Brun and F. Rademakers, ROOT: An object oriented data analysis framework, Nucl. Instrum. Meth. **A389**, 81–86 (1997).

[28] *Pyroot library documentation*, `https://root.cern.ch/pyroot` (visited on 08/17/2018).

[29] *Lhc data interchange protocol*, `https://edms.cern.ch/document/457113/2` (visited on 08/16/2018).

[30] *Central cms-lumi-pog github repository, van der meer analysis framework, pre-automation*, `https://github.com/CMS-LUMI-POG/VdMFramework` (visited on 08/16/2018).

[31] *Bril gitlab repository, van der meer analysis framework, pre-automation branch*, `https://gitlab.cern.ch/bril/VdMFramework` (visited on 08/16/2018).

[32] *Bril gitlab repository, van der meer analysis framework, automation branch*, `https://gitlab.cern.ch/bril/VdMFramework/tree/emit_auto_lite` (visited on 08/16/2018).

[33] *Private github repository of peter tsrunchev, van der meer analysis framework, automation branch*, `https://github.com/peshence/VdMFramework/tree/emit_auto_lite` (visited on 08/16/2018).

[34] *Documentation for pre-automation van der meer analysis framework, by monika grothe*, https://twiki.cern.ch/twiki/pub/CMS/VdMLumiFramework/Tutorial_April2015.pdf (visited on 08/16/2018).

[35] *Some documentation on how to run the updated van der meer analysis framework*, https://twiki.cern.ch/twiki/bin/viewauth/CMS/RunningVdMFramework (visited on 08/16/2018).

[36] *Introducing json*, https://www.json.org/ (visited on 08/17/2018).

[37] The HDF Group, *Hierarchical data format version 5*, http://www.hdfgroup.org/HDF5 (visited on 08/17/2018).

[38] W. McKinney, Pandas: a foundational python library for data analysis and statistics,

[39] *Python 2.7 documentation*, https://docs.python.org/2.7/ (visited on 08/17/2018).

[40] M. Hostettler and G. Papotti, Beam Size Estimation from Luminosity Scans at the LHC During 2015 Proton Physics Operation, MOPMR025. 3 p (2016).

[41] M. Hostettler, K. Fuchsberger, and G. Papotti, Operational Experience with Luminosity Scans for Beam Size Estimation in 2016 LHC Proton Physics Operation, in Proceedings, 8th International Particle Accelerator Conference (IPAC 2017): Copenhagen, Denmark, May 14-19, 2017 (2017), MOPAB109.

Further Bibliography

[2] D. Treille, The experimental challenges of lhc, Journal of Physics: Conference Series **53**, 117 (2006).

[13] W. Herr and B. Muratori, Concept of luminosity, (2006).

[17] O. Karacheban and W. Lohmann, Luminosity measurement at CMS, Presented 05 Jan 2017 (2017).